https://doi.org/10.53655/joe.g2252g

Jurnal OptoElektronik

Demonstration of multiple dissipative solitons with nickel based metal organic framework saturable absorber

Amir Murad[1,2], Norita Mohd Yusoff[1], Josephine Ying Chyi Liew[3], Mohd Hanif Yaacob[1] and Mohd Adzir Mahdi[1*]

[1]*Wireless and Photonics Network Research Centre, Faculty of Engineering, Universiti Putra Malaysia, 43400 UPM Serdang, Selangor, Malaysia*
[2]*FATA University, TSD Dara, NMD Kohat, 26100, Khyber Pakhtunkhwa, Pakistan*
[3]*Department of Physics, Faculty of Science, Universiti Putra Malaysia, 43400 UPM Serdang, Selangor, Malaysia*
Corresponding author: *mam@upm.edu.my

Keywords

Metal-organic framework
saturable absorber
dissipative soliton
pulse mode-locked laser

Article History

Received: 18 August 2022
Accepted: 30 December 2022
Published: 31 December 2022

Abstract

In this work, we have demonstrated the generation of dissipative soliton from single to multi-pulsing phenomenon. The generation of ultrashort pulses was achieved with nickel-based metal organic framework (Ni-MOF) as saturable absorber in a ring cavity erbium-doped fiber laser. The SA was fabricated by spin-coating Ni-MOF/polydimethylsiloxane composite on a tapered fiber substrate, which had an insertion loss of 2.82 dB, a modulation depth of 4.61%, and saturation intensity of 30.12 MW/cm^2. A self-started DS mode-locked pulse was observed at 1559.89 nm central wavelength with 3-dB bandwidth of 19.72 nm at threshold pump power of 33.5 mW. Its pulse width of 7.89 ps was recorded at 7.94 MHz repetition rate. The nature of pulse splitting was observed up to three pulses which were separated with 2.62 ns time spacing with the increment of pump power until 134.2 mW. The generated multiple dissipative soliton pulses realized in the laser cavity through Ni-MOF saturable absorber were stable and invariant for 1-hour stability measurement.

1. Introduction

Ultrashort pulse fiber lasers with compact structure and high power are drawing extensive research interest in both academic and industrial applications [1]. These lasers can be achieved by incorporating a saturable absorber (SA) into the laser cavity. In general, SAs can be classified as real and artificial SAs. The artificial SAs include nonlinear polarization rotation and nonlinear optical loop mirror, which are mainly relied on nonlinear effects in the laser cavity. Besides having the advantages of a high damage threshold, the performance of artificial SAs is affected by large saturation intensity, adversity in self-starting and performance degradation by environmental factors [2].

On the other hand, the real SAs have emerged as an excellent alternative owing to their desired characteristics like compact structure, better stability, broad and tunable bandwidth, and comparatively resistant to environmental perturbation [3]. Therefore, ultrashort pulse fiber lasers realized with real SA have been extensively explored and proven to be an exceptional platform for investigating pulse dynamics [4]. Besides conventional soliton (CS) and noise like pulses (NLP), other nonlinear phenomena can also be investigated using the real SAs [5].

Up to date, various operation regimes have demonstrated different pulse dynamics [6]. A mode-locked fiber laser with characteristics of CS can be obtained by adjusting the dispersion and nonlinearities in an anomalous dispersion regime. The CS is characterized by Kelly sidebands whose energy is limited owing to the soliton area theorem [7]. On the other hand, the mode-locked stretched pulse can be attained in the dispersion-managed region, where its pulse energy is considerably increased and vice-versa for peak power [8]. To further increase the pulse energy, dispersion engineering is necessary to operate a mode-locked laser in a normal dispersion regime, where dissipative soliton (DS) can be formed. The DS is different from CS, where the pulse formation is also dependent on the cavity gain and loss as well as spectral filtering effect [9]. This condition is necessary for a stable performance of the laser. Thus, a composite balance of nonlinearities, dispersion, gain, loss and spectral filtering effect is required to achieve DS mode-locked operation and extend the allowed pulse energy. Moreover, it also instigates the DS optical spectrum to possess step edges with a flat top exhibiting a near square profile, its characteristic feature [10]. However, the

pulse energy is still limited by the event of multi-pulsing with the increment of pump power. The research on the DS system is reasonably sufficient; however, the reports on multi-pulsing and its relationship with pump power are comparatively inadequate and need to be explored further.

In this work, the generation of DS in erbium-doped fiber laser using nickel-based metal organic framework (Ni-MOF) SA was experimentally demonstrated. The Ni-MOF was synthesized by solvothermal method utilizing $Ni(NO_3)_2.6H_2O$ as metal cations and trimesic acid as ligand. The Ni-MOF SA possesses the desired properties to realize DS generation. We observed the evolution of DS pulse to its multi-pulse during pump power development. The single and multi-pulse operations were stable for 1-hour stability measurement. The work will add to the understanding of DS pulse evolution and multiple pulses formation.

2. Fabrication and characterization of SA

The SA was fabricated using tapered fiber as an optical platform. It was fabricated by tapering single-mode fiber (SMF) with specific dimensions via a Vytran GX-3400 workstation. The tapered fiber with an up/down taper of 30 mm, a waist-length of 0.8 mm and a waist diameter of 10 μm was fabricated. The details on materials, synthesis and characterization have been explained in our previous work [11]. The sample, synthesized with a traditional solvothermal method having a metal to ligand ratio of 2:1, was further used for DS pulse generation in this work. The material for SA preparation was processed by sonicating 0.3 mg of Ni-MOF in a beaker containing 10 ml of isopropyl alcohol (IPA). Next, 1 g of polydimethylsiloxane (PDMS), a low absorption polymer was added to the well dispersed Ni-MOF solution mixture. This solution mixture was then put on a hot plate magnetic stirrer at 82°Cuntil the IPA evaporated. Afterward, 0.1 g of curing agent was mixed to the Ni-MOF and PDMS composite solution, which was stirred with a glass rod to ensure homogenous composite materials distribution. For the fabrication of SA, the as-prepared material was then spin-coated on the tapered fiber with spinning parameters of 4000 rpm for 5 minutes.

The fabricated SA was then characterized for insertion loss and nonlinear optical properties. The insertion loss was measured using a broadband amplified spontaneous emission source. Figure 1(a) depicts the insertion loss of materials, which illustrates 2.82 dB loss at 1560 nm. The nonlinear properties were evaluated through nonlinear transmission properties measured through a balanced twin detector measurement system as employed in our research group [12]. The transmission increases initially with increasing input optical intensity and is then saturated at specific input power called a saturable absorption phenomenon, as shown in Figure 1(b). The prepared SA had a modulation depth (MD) of 4.61% and a saturation intensity (I_{sat}) of 30.12 MW/cm^2.The transmission decreased gradually by further increasing the input power, illustrating the reverse saturable absorption (RSA) effect. The RSA may be due to the two-photon absorption and scattering effects [12]. The estimated two-photon absorption coefficient of 7.7×10^{-4} cm^2/MW was obtained with fabricated SA calculated from a nonlinear saturable absorption curve.

3. Cavity setup

An erbium-doped fiber laser (EDFL) was constructed to generate mode-locked DS pulses using Ni-MOF-based SA. The schematic of the laser cavity configuration is shown in Figure 2. The cavity was pumped with a 980 nm laser diode (LD) through a 980/1550 nm wavelength division multiplexer (WDM). A 13 m length of erbium-doped fiber (EDF) was employed as a gain medium having a dispersion coefficient of 23 ps^2/km. A polarization-independent isolator was incorporated after EDF to circumvent the back reflection of propagating light and ensure the unidirectional oscillation of the laser cavity. The as-prepared SA was inserted between the isolator and polarization controller (PC) to initiate and stabilize the mode-locking operation. A 50:50 output coupler was utilized to extract 50% of EDFL output from the cavity for performance analysis. The cavity was constructed from three types of fiber, i.e., EDF, SMF and Hi-1060, having 15, 10 and 2.35 m length, respectively. The corresponding net group velocity dispersion (GVD) calculated for the EDFL ring cavity was 0.115 ps^2, which validates the operation in a normal dispersion regime.

4. Results and discussion

The evolution of laser output spectrum with increasing pump power up to 134.2 mW was measured through an optical spectrum analyzer (OSA) as portrayed in Figure 3(a). The continuous wave (CW) lasing threshold was attained at 13.7 mW pump power. Further increment of the pump power to 33.4 mW, a self-started mode-locking state was reached. The mode-locked laser generated a DS pulse characterized by a flat top and steep edges, as illustrated in Figure 3(b). The corresponding 3-dB bandwidth of 19.72 nm and central wavelength of 1559.89 nm were observed for the optical spectrum recorded at the mode-locked threshold. The oscilloscope pulse train as shown

https://doi.org/10.53655/joe.g2252g

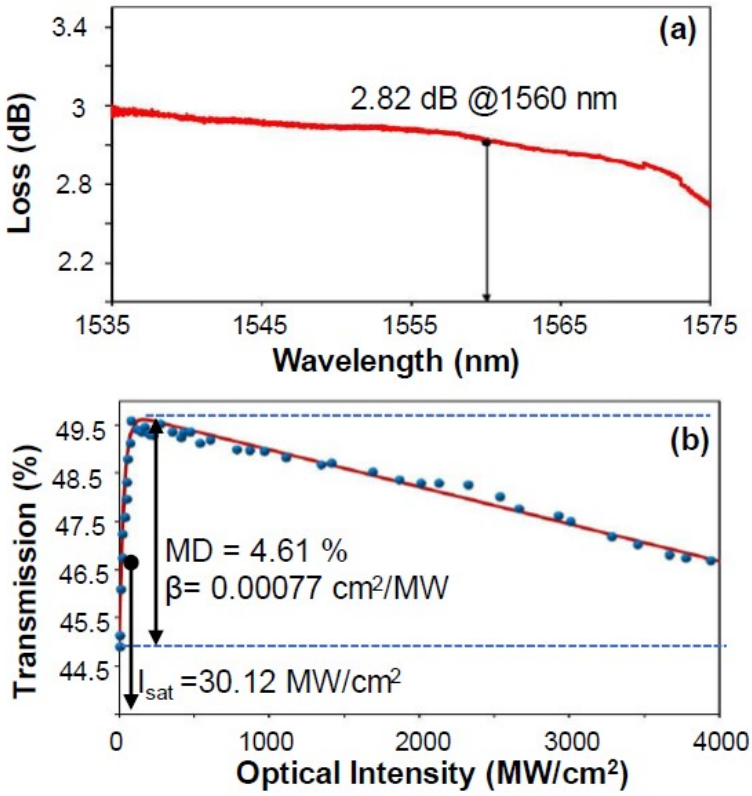

Figure 1. (a) Transmission loss and (b) nonlinear saturable absorption curve of Ni-MOF SA

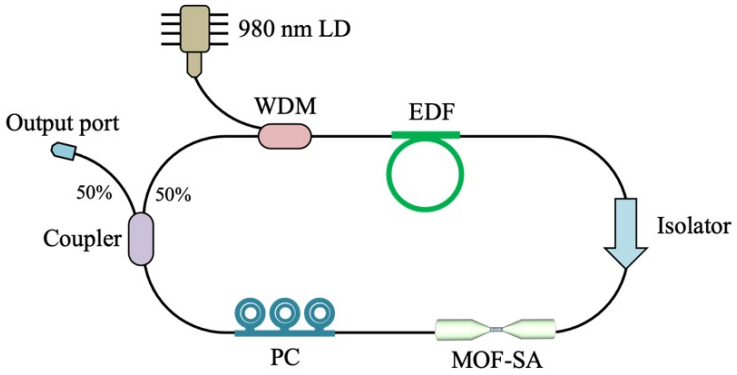

Figure 2. Schematic of EDFL ring cavity integrated with Ni-MOF SA

in Figure 3(c), illustrates uniform intensity having a pulse interval of 126 ns, which corresponds to the fundamental repetition rate of 7.94 MHz. An autocorrelation trace and its Gaussian fitting are illustrated in Figure 3(d), which shows a full width at half maximum (FWHM) of 11.12 ps. Then, its pulse width of 7.89 ps was obtained after deconvolution. The time-bandwidth product (TBP) calculated from the 3-dB bandwidth, central wavelength and pulse width was 19.18, which was high compared to the transform-limited pulse confirming the generated DS pulse was severely chirped. As depicted in Figure 3(e), the RF spectrum demonstrates signal-to-noise ratio (SNR) of 53.85 dB, indicating a stable mode-locked pulse was realized in the EDFL cavity. Moreover, the RF spectrum was observed at a fundamental repetition rate of 7.94 Mhz confirming the oscilloscope measurement (refer to Figure 3(c)). It is worth mentioning that by increasing pump power until 74 mW, a single-pulse operating at fundamental repetition rate was maintained.

By increasing the pump power further to 75.6 and 96.5 mW, dual- and triple-pulse operations were attained as illustrated in Figure 4. The switching of fundamental pulse to multiple pulses might be due to the two-photon absorption, which leads to peak limiting and soliton quantization effect on mode-locked DS pulse [13]. In fact, an SA

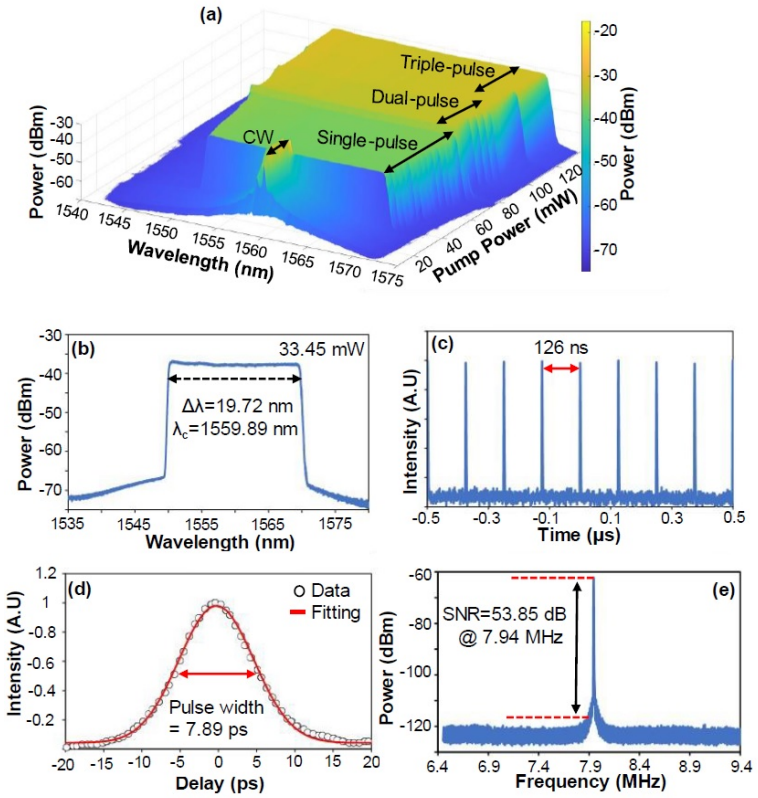

Figure 3. (a) Power development spectrum, (b) mode-locked spectrum at 33.45 mW, (c) oscilloscope pulse train, (d) autocorrelator pulse trace, and (e) RF spectrum of DS pulse generated from the EDFL with Ni-MOF SA

with high MD is required to maintain single pulse operation in the net positive GVD laser cavity. The occurrence of two-photon absorption in the laser cavity reduced the effective MD and nonlinear transmission curve of the Ni-MOF SA, which caused the switching effect from single to multi-pulse operation regime to achieve pulse stabilization. A uniform pulse interval of 2.62 ns was observed between adjacent double pulses as illustrated in inset of Figure 4(a), whereas a pulse interval of 2.62 ns was observed between the neighbouring pulses in the three-pulse operation as illustrated in inset of Figure 4(c). It is important to highlight that the time interval between the second and third pulse were maintained at 126 ns (fundamental repetition rate). As illustrated in Figure 4(b,d), the optical spectrum of these dual- and triple-pulse were broadened as compared to single DS pulse. The 3-dB bandwidth of 23.36 and 23.66 nm were recorded at the pump power of 75.6 and 96.5 mW, respectively. Similarly, the central wavelengths observed during power development varied marginally, with an average value of 1559.77 nm and a standard deviation of 0.12 nm. The optical spectrums still depict a flat top with steep edges during power development, even when the oscilloscope traces split into two and three pulses.

Figure 5 portrays the trend of 3-dB bandwidth of the laser output in relation to the pump power. It can be seen that the initial value of 19.72 nm (refer to Fig. 3(b)) was obtained at the threshold pump power. The single pulse operation existed until 74 mW pump power whereby the 3-dB bandwidth grew from 19.72 to 22.30 nm. Then, the single pulse broke to two pulses up to 95.6 mW pump power. For the dual-pulse case, the 3-dB bandwidth in the range of 21.70–23.36 nm was recorded. Beyond this pump power, a new pulse was generated to form triple-pulse operation in the laser cavity up to 134 mW. In this phase, the 3-dB bandwidth varied from 22.3 to 23.9 nm. From the experiment, it is known that the enlargement of spectral bandwidth is due to the effect self-phase modulation [14]. However, this effect is relied on the peak power of individual pulses in the laser cavity. When the pulse breaks up, the peak power is halved and therefore, the broadening effect is reduced. Then, the two pulses gain its peak power when the pump power is pushed to the higher value. This effect is regulated at the point of pulse breaking transition, which occurred twice in our experiment. The maximum average output power of 7.54 mW and pulse energy of 0.94 nJ were obtained from the mode-locked EDFL cavity.

For DS laser systems, it is a known issue that the stability of these multiple pulses is of grave concern, where multiple pulses are either varied or vanished during the observation time [8]. From this experimental work, we

https://doi.org/10.53655/joe.g2252g

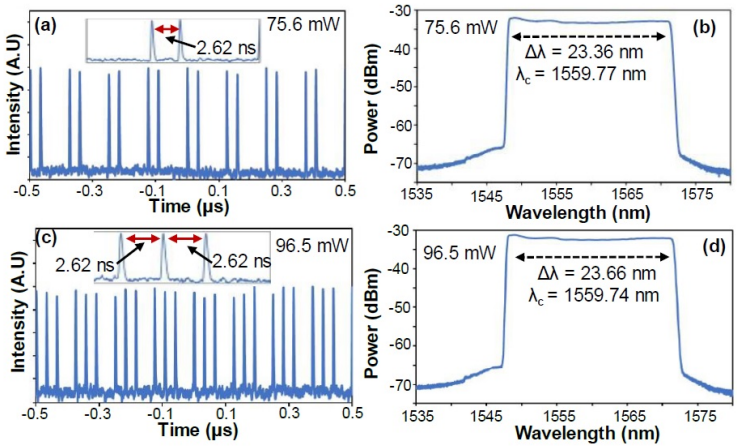

Figure 4. Oscilloscope pulse train and optical spectrum of dual-pulse DS [(a), (b)], and triplepulse DS [(c) and (d)]

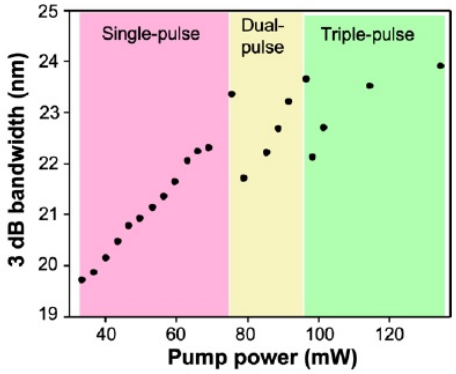

Figure 5. Evolution of 3 dB bandwidth as a function of pump power for all phases of DS operations

set three different operational regimes; single-, dual- and triple-pulse. The optical spectrum and oscilloscope trace were recorded for every 10 minute interval for an hour time. All traces from this experiment were plotted as shown in Figures 6 and Figure 7. Overall, all the recorded optical spectra maintained a flat top with steep edges during the stability measurement. Conversely, the oscilloscope traces of single and multiple pulses observed in this work were steady and time-invariant pulses, as observed in the operational stability measurement shown in Figure 6. This phenomenon was also observed in [15], where the pulse was split into multiple DS pulses with equal and invariant temporal pulse spacing. The stability and variances of single and multiple DS pulses was further justified through optical spectrums stability measurement. The corresponding 3-dB bandwidth and central wavelength were also measured for each spectrum and plotted in Figure 7(d-f). The standard deviation value of central wavelength for all pulses was less than or equal to 0.5 nm. On the other hand, for the 3-dB bandwidth, the maximum standard deviation of 0.15 nm was observed in three-pulse stability measurement. Moreover, the stability spectrum recorded through an oscilloscope, as illustrated in Figure 6, further confirms that these pulses are stable and invariant during stability measurement.

5. Conclusion

In conclusion, we have experimentally demonstrated the evolution of mode-locked DS from single pulse to multiple pulses by increasing pump power in the laser cavity. The optical spectrum, characteristic of DS pulse with flat top and steep edges, was observed during the experiment from the mode-locked threshold power of 33.4 mW until 134.2 mW maximum pump power. For the single-pulse operation, the proposed laser generated DS mode-locked pulse at 1559.89 nm central wavelength, 19.72 nm spectral bandwidth, 7.89 ps pulse width, and 7.94 MHz repetition rate. The evolution of pulse splitting occurred at 75.6 and 96.5 mW pump power that triggered the dual- and triple-pulse operations, respectively. All the pulses were time invariant and stable without any observable change

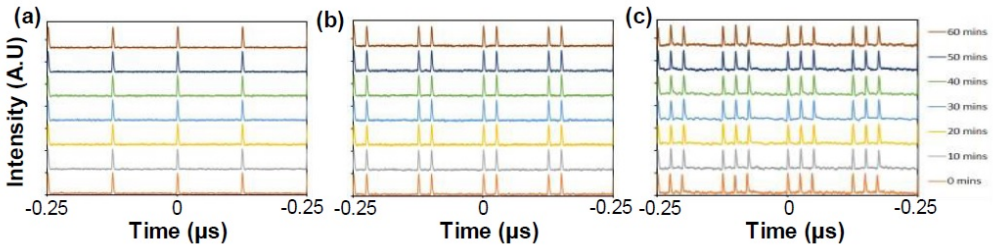

Figure 6. Evolution of oscilloscope traces during stability measurement (a) single-, (b) dual- and (c) triple-pulse DS operations

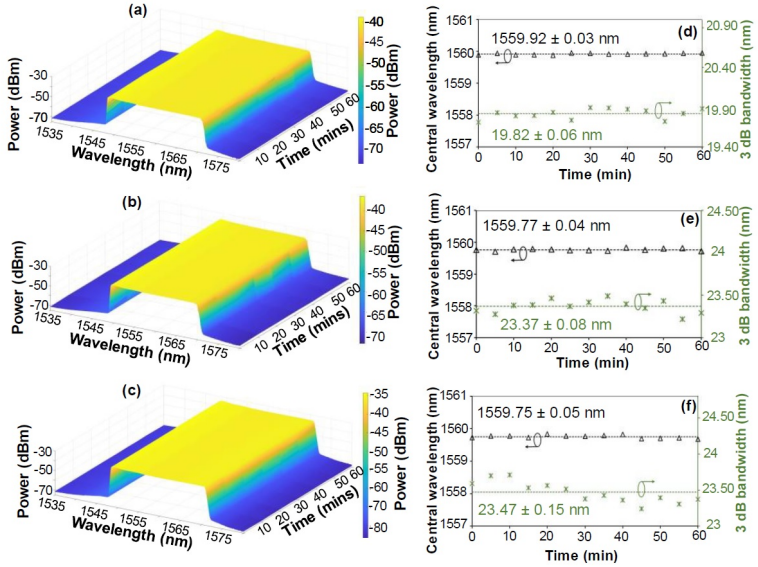

Figure 7. Optical spectrum evolution for 1-hour stability measurement of (a) single-, (b) dual-, (c) and triple-pulse DS operations. Their corresponding 3-dB bandwidth and central wavelength variations during the stability measurement for (d) single-, (e) dual-, and (f) triple-pulse DS operations

for an hour stability measurement. This was verified by small value of standard deviation for central wavelength and its 3-dB bandwidth.

Acknowledgement

This work was supported by the Collaborative Research in Engineering, Science and Technology (CREST) under the Open R&D Grant P07C1-19.

References

[1] Y. Han, Y. Guo, B. Gao, C. Ma, R. Zhang, and H. Zhang, "Generation, optimization, and application of ultrashort femtosecond pulse in mode-locked fiber lasers," *Progress in Quantum Electronics*, vol. 71, p. 100 264, May 2020. DOI: 10.1016/j.pquantelec.2020.100264.

[2] S. M. Kobtsev, "Artificial saturable absorbers for ultrafast fibre lasers," *Optical Fiber Technology*, vol. 68, p. 102 764, Jan. 2022. DOI: 10.1016/j.yofte.2021.102764.

[3] K. Y. Lau and D. Hou, "Recent research and advances of material-based saturable absorber in mode-locked fiber laser," *Optics & Laser Technology*, vol. 137, p. 106 826, May 2021. DOI: 10.1016/j.optlastec.2020.106826.

[4] C. Lv, H. Luo, L. Cui, *et al.*, "Silver nanowires with ultrabroadband plasmon response for ultrashort pulse fiber lasers," *Advanced Photonics Research*, vol. 3, no. 1, p. 2 100 184, Oct. 2021. DOI: 10.1002/adpr.202100184.

https://doi.org/10.53655/joe.g2252g

[5] B. Wang, H. Han, L. Yu, Y. Wang, and C. Dai, "Generation and dynamics of soliton and soliton molecules from a VSe_2GO-based fiber laser," *Nanophotonics*, vol. 11, no. 1, pp. 129–137, Nov. 2021. DOI: 10.1515/nanoph-2021-0543.

[6] C. Huang, C. Wang, W. Shang, N. Yang, Y. Tang, and J. Xu, "Developing high energy dissipative soliton fiber lasers at 2 micron," *Scientific Reports*, vol. 5, no. 1, Sep. 2015. DOI: 10.1038/srep13680.

[7] H.-J. Chen, M. Liu, J. Yao, *et al.*, "Buildup dynamics of dissipative soliton in an ultrafast fiber laser with net-normal dispersion," *Optics Express*, vol. 26, no. 3, p. 2972, Jan. 2018. DOI: 10.1364/oe.26.002972.

[8] L.-N. Duan, J. Wen, W. Fan, and W. Wang, "Generation of single and multiple dissipative soliton in an erbium-doped fiber laser," *Chinese Physics B*, vol. 26, no. 10, p. 104 205, Sep. 2017. DOI: 10.1088/1674-1056/26/10/104205.

[9] N. Akhmediev, J. M. Soto-Crespo, P. Vouzas, N. Devine, and W. Chang, "Dissipative solitons with extreme spikes in the normal and anomalous dispersion regimes," *Philosophical Transactions of the Royal Society A: Mathematical, Physical and Engineering Sciences*, vol. 376, no. 2124, p. 20 180 023, Jun. 2018. DOI: 10.1098/rsta.2018.0023.

[10] Y. Song, X. Shi, C. Wu, D. Tang, and H. Zhang, "Recent progress of study on optical solitons in fiber lasers," *Applied Physics Reviews*, vol. 6, no. 2, p. 021 313, Jun. 2019. DOI: 10.1063/1.5091811.

[11] A. Murad, J. Y. C. Liew, M. H. Yaacob, *et al.*, "Effect of nickel ion concentration on structural, optical and electrical properties towards Ni-H_3BTC-MOF formation for nonlinear saturable absorption phenomenon," *Journal of Physics and Chemistry of Solids*, vol. 167, p. 110 743, Aug. 2022. DOI: 10.1016/j.jpcs.2022.110743.

[12] M. A. W. A. Hadi, K. Y. Lau, N. M. Yusoff, *et al.*, "Nano-tungsten trioxide saturable absorber for l-band noise-like pulse mode-locked fiber laser," *Optical Fiber Technology*, vol. 71, p. 102 933, Jul. 2022. DOI: 10.1016/j.yofte.2022.102933.

[13] Q. Wang, Y. Chen, L. Miao, *et al.*, "Wide spectral and wavelength-tunable dissipative soliton fiber laser with topological insulator nano-sheets self-assembly films sandwiched by PMMA polymer," *Optics Express*, vol. 23, no. 6, p. 7681, Mar. 2015. DOI: 10.1364/oe.23.007681.

[14] U. Brauch, C. Röcker, T. Graf, and M. A. Ahmed, "High-power, high-brightness solid-state laser architectures and their characteristics," *Applied Physics B*, vol. 128, no. 3, Mar. 2022. DOI: 10.1007/s00340-021-07736-0.

[15] M. A. Abdelalim, Y. Logvin, D. A. Khalil, and H. Anis, "Steady and oscillating multiple dissipative solitons in normal-dispersion mode-locked yb-doped fiber laser," *Optics Express*, vol. 17, no. 15, p. 13 128, Jul. 2009. DOI: 10.1364/oe.17.013128.